Geophys. J. Int. (2004) **157,** 1377–1392 doi: 10.1111/j.1365-246X.2004.02270.x

Contemporary kinematics of the southern Aegean and the Mediterranean Ridge

Corné Kreemer[1]* and Nicolas Chamot-Rooke[1,2]

[1]*Laboratoire de Géologie, Ecole normale supérieure, Paris, France; E-mail: kreemer@cdf.u-3mrs.fr*
[2]*CNRS UMR* 8538*. E-mail: rooke@geologie.ens.fr*

Accepted 2004 February 16. Received 2004 January 14; in original form 2003 January 31

SUMMARY

This study focuses on the kinematics of the southern Aegean and the Mediterranean Ridge (MR). A quantification of the deformation of the MR is essential for both evaluating physical models of accretionary wedges in general and for obtaining a self-consistent model of the surface deformation over the entire Nubia–Eurasia (NU–EU) plate boundary zone in the eastern Mediterranean. Previous kinematic studies have not properly considered the deformation field south of the Hellenic arc. Although this study focuses on the deformation field of the MR, we also discuss the kinematics of the southern Aegean, because the geometry and movement of the Hellenic arc determine to a large extent the kinematic boundary conditions for kinematic studies of the MR. We calculate a continuous velocity and strain rate field by interpolating model velocities that are fitted in a least-squares sense to published Global Positioning System (GPS) velocities. In the interpolation, we use information from a detailed data set of onshore and offshore active faulting to place constraints on the expected style and direction of the model strain rate field. In addition, we use the orientations of tracks left by seamounts travelling into the wedge to further constrain the offshore deformation pattern. Our model results highlight the presence of active shear partitioning within the Mediterranean ridge. High compressional strain rates between the ridge crest and the deformation front accommodate approximately 60–70 per cent of the total motion over the wedge, and the outward growth rate of the frontal thrust is ~ 4 mm yr^{-1}. Strain partitioning within the wedge leads to 19–23 mm yr^{-1} of dextral motion at the wedge–backstop contact of the western MR, whereas the Pliny and Strabo trenches in the eastern MR accommodate 21–23 mm yr^{-1} of sinistral motion. The backstop of the western MR is kinematically part of the southern Aegean, which moves as a single block [the Aegean block (AE)] at 33–34 mm yr^{-1} in the direction of S24°W $\pm$ 1° towards stable Nubia (NU). Our model confirms that there is a clear divergence between the western and eastern Hellenic arc and we argue for a causal relation between the outward motion of the arc and the gradient in the regional geoid anomaly. Our results suggest that a significant driving source of the surface velocity field lies south of the Hellenic arc and only for the southeastern Aegean could there be some effect as a result of gravitational collapse associated with density differences within the overriding plate.

Key words: Aegean, crustal deformation, Global Positioning System (GPS), Mediterranean ridge, tectonics, plate convergence.

1 INTRODUCTION

A common consensus on most of the present-day deformation field in the eastern Mediterranean has been reached only recently, after horizontal crustal motions have been measured extensively using space-geodetic techniques, particularly the Global Positioning System (GPS) (Billiris *et al.* 1991, Noomen *et al.* 1993; Straub & Kahle 1994; Kahle *et al.* 1995; Davies *et al.* 1997; Reilinger *et al.* 1997; Clarke *et al.* 1998; Cocard et al. 1999; Briole *et al.* 2000; McClusky *et al.* 2000; Ayhan et al. 2002; Meade *et al.* 2002). Two thorough overview studies (Kahle *et al.* 2000; McClusky *et al.* 2000), as well as all the mentioned geodetic studies, have provided valuable contributions to our understanding of eastern Mediterranean tectonics and the geodynamic implications. However, no study has implicitly addressed the deformation field south of the Hellenic arc. This is

*Now at Collège de France, Chaire Géodynamique, Europôle de l'Arbois, BP 80, Bat. Laennec, Hall D 13545, Aix en Provence, France

partly out of necessity, because there are no islands south of the Arc (except Gavdos) and thus no geodetic measurements, partly out of ignorance or the need for simplicity and partly as a result of history. The historic inclination has been to consider the Hellenic Trench (just south of the arc) as the main plate boundary. Recent kinematic models have assumed the region south of the trench either to be part of Africa (e.g. Jackson *et al.* 1994; Nyst 2001) or to deform uniformly (e.g. Kahle *et al.* 2000). Yet, this region is dominated by the actively deforming and growing Mediterranean Ridge (MR) accretionary wedge, and a description of its deformation field, as part of the entire plate boundary zone deformation, is still lacking.

Although no geodetic measurements have been possible between the Hellenic arc and northern Africa, the existing GPS velocities provide important boundary conditions to study the offshore kinematics. These boundary conditions can be identified by three main characteristics. First, the convergence rate reaches a maximum of approximately 3 cm yr^{-1} between Crete and the Cyrenaica promontory (Libya) and decreases significantly towards the Calabrian and Cyprus arcs in the west and east, respectively (McClusky *et al.* 2000). Secondly, a radial component with respect to the inner Aegean exists in the GPS velocity field along the eastern branch of the Hellenic arc (McClusky *et al.* 2000). Thirdly, plate velocities are highly oblique to the trend of the Hellenic arc and this observation was one of the arguments from which Le Pichon *et al.* (1995) proposed that strain partitioning occurs. Moreover, the rapid lateral change of the trend of the Hellenic Arc near Crete predicts an opposite sense of shear offshore the western (Ionian) and eastern (Herodotus) branches of this arc.

The MR comprises most of the region between the Hellenic trench and Africa, and terminates near the Calabrian arc in the west and south of Anatolia in the east. It is now well established that the MR is a large accretionary wedge of Neogene sediments and Messinian evaporites, and is created by the ongoing subduction of Africa underneath the Aegean (e.g. Biju-Duval *et al.* 1978; Le Pichon *et al.* 1982; Ryan *et al.* 1982; Kastens 1991; Truffert *et al.* 1993; Chaumillon & Mascle 1997). Since the middle Miocene, when initiation of accretion took place, the wedge has grown to be more than 10 km thick and over 200 km wide. Recent overviews of the structure and evolution of the wedge and backstop are presented elsewhere (Fruehn *et al.* 2002; Reston *et al.* 2002). This paper draws most of its inferences and input on the tectonics and geometry of the MR from a paper submitted by N. Chamot-Rooke et al. entitled 'Active tectonics of the Mediterranean Ridge' and hereafter referred to as Chamot-Rooke *et al.* (2004).

The aim of this paper is to establish a self-consistent kinematic model of the surface deformation of the MR. We implicitly consider the deformation of the MR accretionary wedge in a description of the surface deformation of the Africa–Aegean plate boundary zone and at the same time we are not concerned with the deformation at depth. In order to obtain our model we use the geodetic velocities as boundary conditions and include other tectonic information (discussed below) to further constrain the horizontal deformation field. Particularly, our models are obtained from an inversion of the regional GPS velocities and incorporate plate boundary velocity constraints on the rigid plates adjacent to the eastern Mediterranean deformation zone. For our preferred model we include additional constraints on the style and direction of expected strain rates inferred from a new map of active onshore and offshore faulting. Furthermore, we use track directions of seamounts (and other surface relief) that travel into the wedge as extra constraints. We illustrate the significance of the inclusion of offshore kinematic data on the regional kinematics. In this paper, we also discuss briefly the southern Aegean (comprising the Hellenic arc, Peloponnesus, Cyclades and the sea of Crete) because the kinematics of the MR can only be understood properly by adopting the backstop as a reference frame and understanding its motion in terms of a velocity boundary condition. Although we could have used existing models for the southern Aegean kinematics (McClusky *et al.* 2000), we prefer to model the entire area simultaneously in order to be self-consistent and to have the ability to include multiple complementary GPS studies in a consistent reference frame.

We predict present-day horizontal-velocity and strain rate fields. We examine the role and extent of strain partitioning, place bounds on the deformation style and rates of structures observed along the MR, try to place constraints on the growth rate of the wedge and evaluate the crustal flow field of the combined southern Aegean and MR. We also briefly discuss the extent, rigidity and motion of the Aegean block (AE) and its continuation with the wedge backstop. Finally, we discuss the possible implications of our new kinematic model for the dynamics of the region.

2 DATA

2.1 Geodetic velocities

A very large number of GPS velocities are available for the Aegean and eastern Mediterranean. We use vectors (Fig. 1) from the following studies: west-central Greece (Kahle *et al.* 1995); central Greece/Corinth gulf (Clarke *et al.* 1998); western Hellenic arc (Cocard *et al.* 1999); Greece and Turkey (McClusky *et al.* 2000); Bulgaria (Kotzev *et al.* 2001); north-west Turkey (Ayhan *et al.* 2002; Meade *et al.* 2002). Not all velocities were used, as discussed in Appendix A. In Appendix A, we also discuss the uncertainties in the observed GPS vectors. For the study presented here only the studies by Kahle *et al.* (1995), Cocard *et al.* (1999) and McClusky *et al.* (2000) are of direct importance. The implications of the result of the latter study on our modelling efforts have already been discussed in the introduction, whereas the former two studies have supplied important constraints on the motion of the western Hellenic arc and the localization of strain along the Kephalonia fault, being the northwestern continuation of the MR.

All the incorporated geodetic studies have presented velocity estimates in their own specific reference frame. To rotate all vectors in a consistent model Eurasia (EU) reference frame, the velocities of the studies above were placed in a version of the global model of Kreemer *et al.* (2003) that was particularly designed for this study. In there, we make the approximate assumption that the difference between the reference frames consists solely of a rigid body rotation (i.e. translation and scale factors are ignored, which are generally of insignificant impact for regional studies (Kreemer *et al.* 2003)). We solve for this rigid body rotation for each study (and subsequently apply the rotation to the velocity vectors) in the process of obtaining a best fit between observed and model velocities in a EU reference frame (Table 1). Subsequently, all vectors of the above studies within a fixed EU reference frame were used in the regional study presented here. In practice, this approach implies that the obtained rotation between the published EU frame of McClusky *et al.* (2000) and the global model EU frame is well-constrained (and small) because it is determined by minimizing the misfit between their velocities on stable Eurasia and the ∼100 velocities for stable Eurasia published elsewhere. All velocities of other studies in the Aegean (that do not report velocities on stable Eurasia) then merely rotate into an EU reference frame in a way that the differences between those velocities and those by McClusky *et al.* (2000) are minimized.

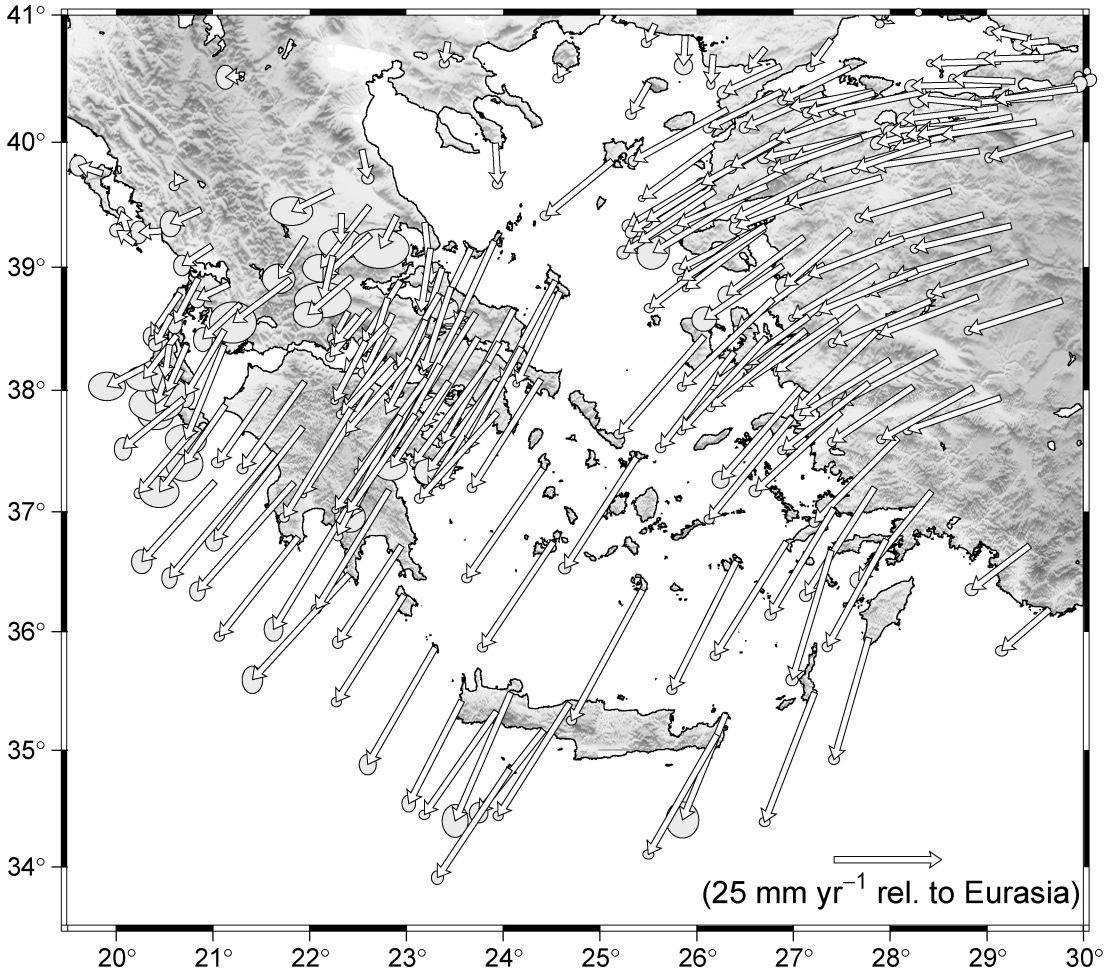

Figure 1. GPS velocities in the greater Aegean used in this study. Velocities are in a model Eurasia reference frame and error ellipses represent $1-\sigma$ uncertainties. Velocities are taken from Kahle *et al.* (1995), Cocard *et al.* (1999), McClusky *et al.* (2000), Clarke *et al.* (1998), Meade *et al.* (2002), and Ayhan *et al.* (2002). This figure is in colour in the online version where each color indicates a different study: grey, Kahle *et al.* (1995); yellow, Cocard *et al.* (1999); red, McClusky *et al.* (2000); green, Clarke *et al.* (1998); light blue, Meade *et al.* (2002); orange, Ayhan *et al.* (2002).

Table 1. Angular velocities obtained and used to rotate original GPS velocities in a model EU reference frame.

Study	Lat. °N	Long. °E	ω° Myr^{-1}	σ_{max}	σ_{min}	ζ_{max}	σ_ω
Ayhan *et al.* (2002)	38.4	34.4	0.310	0.5	0.3	−71	0.068
Clarke *et al.* (1998)	46.8	26.6	0.226	2.6	0.8	31	0.255
Cocard *et al.* (1999)	31.6	21.4	0.091	0.6	0.4	83	0.083
Kahle *et al.* (1995)	33.2	25.4	−0.416	11.8	3.2	53	0.309
Kotzev *et al.* (2001)	48.1	17.2	−0.067	3.2	1.7	49	0.093
McClusky *et al.* (2000)	39.4	15.2	−0.022	2.6	2.6	−17	0.008
Meade *et al.* (2002)	39.8	33.2	0.176	0.9	0.4	89	0.071

All studies had published velocities in their defined Eurasian (EU) reference frame, except Kahle *et al.* (1995) who reported velocities relative to the MATE station.
$1-\sigma$ error ellipse axes are in degrees and ζ_{max} is azimuth of maximum axis. For 95 per cent confidence multiply standard errors by 2.45.

2.2 Velocity boundary constraints

To constrain the rigid body motion of the plates adjacent to the eastern Mediterranean plate boundary zone [e.g. Nubia and Arabia] we used the relative angular velocities from an updated version of the global kinematic model of Kreemer *et al.* (2003) (Table 2). For the results presented here, it is important to note that earlier GPS studies (McClusky *et al.* 2000) as well as all available kinematic models based on GPS measurements (i.e. Kreemer & Holt 2001; Sella *et al.* 2002; Calais *et al.* 2003; Fernandes *et al.* 2003; Kreemer *et al.* 2003; McClusky *et al.* 2003) find that the geodetically-derived present-day NU–EU motion is significantly slower (and directed more westwards along its northern margin) than the estimate of the NUVEL-1A geological model (DeMets *et al.* 1994). This is

Table 2. Relative plate angular velocities used as plate boundary velocity constraints and obtained in this study.

Plate pair	Lat. °N	Long. °E	ω° Myr^{-1}	Reference
Constrained				
NU/EU	4.2	−19.7	0.062	Kreemer *et al.* (2003)[1]
AR/EU	25.9	14.2	0.347	Kreemer *et al.* (2003)[1]
Obtained in this study and previously by others				
AT/EU	30.9	33.0	1.206	This study[2]
AT/EU	30.7	32.6	1.2	McClusky *et al.* (2000)
AE/EU	−43.4	128.9	0.333	This study[3]
AE/EU	−27.8	95.2	0.3	McClusky *et al.* (2000)
AE/NU	−38.2	135.1	0.377	This study

Anatolia (AT); Eurasia (EU); Aegean block (AE); Nubia (NU; Africa); Arabia (AR)

[1]We used an update from the published angular velocities by Kreemer *et al.* (2003)

[2]$1-\sigma$ error ellipse: $\sigma_{max} = 0.3^\circ$, $\sigma_{min} = 0.1^\circ$, $\zeta_{max} = -1^\circ$ and $\sigma_\omega = 0.042^\circ$ Myr^{-1}

[3]$1-\sigma$ error ellipse: $\sigma_{max} = 11.8^\circ$, $\sigma_{min} = 0.4^\circ$, $\zeta_{max} = -69^\circ$ and $\sigma_\omega = 0.043^\circ$ Myr^{-1}

consistent with an actual slowing down in relative plate motion (Calais *et al.* 2003) and probably not the result of the fact that NUVEL-1A considers a single African plate and does not distinguish between an independent Nubia and Somalian plate, west and east of the East African rift, respectively. In the eastern Mediterranean, the model by Kreemer *et al.* (2003) predicts 5–6 mm yr^{-1} of NU–EU convergence rate, which implies a convergence rate between Nubia and the Hellenic arc that is approximately 4 mm yr^{-1} slower than if we had adopted NUVEL-1A as a velocity boundary constraint.

2.3 Geological data

For this study, we make use of a regional geological map produced by the DOTMED Group at Ecole Normale Supérieure that is mainly based on offshore studies of active faulting (Chamot-Rooke *et al.* 2001; Fig. 2). Data from recent cruises were also used for the deep offshore, including the Rhodes basin and eastern MR (Woodside *et al.* 2000; Huguen *et al.* 2001), Ionian basin, Calabrian wedge and western MR (Chamot-Rooke *et al.* 2004), and the Kephalonia fault zone (Nielsen 2003). Note that only the faults inferred to be south of the Hellenic arc are of significant importance to the present study. For all the identified active faults, the principal style of faulting (normal, reverse, strike-slip, or any intermediate) has been determined (Fig. 2). We do acknowledge that for some faults it is difficult to infer whether they are active at present. For onshore areas, GPS velocities are often available for stations sufficiently dense enough to dictate which faults are required to be active and which ones can be considered as inactive. It is of course much more difficult to identify active faults at sea. However, for this purpose we use up-to-date structural mapping based on multibeam surveys and seismic profiling to infer activity in the best possible manner.

2.4 Seamount tracks

Seamounts travelling with the downgoing plate leave a clear indentation track in the accretionary wedge as the downgoing plate subducts (e.g. von Huene *et al.* 1997; Fisher *et al.* 1998; Park *et al.* 1999). The tracks can generally be interpreted as flow lines of relative motion between the overriding and downgoing plates. In the eastern Mediterranean, several seamounts and other highs, such as ridges, have left a measurable track in the actively growing wedge of the western MR. A well-studied track was formed by a seamount that is now buried underneath the Bannock basin (e.g. von Huene *et al.* 1997; Chamot-Rooke *et al.* 2004) (Fig. 2). The Bannock track is 42 km long and has a bearing of approximately N60°E ± 5° (all uncertainties given in this paper are $1-\sigma$), which is approximately normal to the local trend of the wedge toe but significantly more eastwards from the expected direction of the motion between Cyrenaica and the backstop (∼N25°E). Between the Bannock basin and Cyrenaica there exist two other tracks: one track is formed by the Battos mount and has a bearing of N55°E ± 5°, and another is formed by the Akhdar ridge and oriented N35°E ± 10° [Chamot-Rooke *et al.* (2004); Fig. 2]. The orientation of the Battos and Akhdar tracks is oblique to both the trend of the deformation front and the expected backstop–Cyrenaica relative motion. For all surface tracks, it is only possible to infer the direction of local convergence, not the rate. These convergence directions can however be used as kinematic indicators if one assumes that the finite strain direction preserved by the tracks is consistent with present-day convergence direction. Particularly for the Battos and Akhdar tracks, which currently cut through the wedge toe, such an assumption seems valid.

All tracks indicate the local convergence direction and as such they provide the evidence that strain partitioning is occurring in the western MR (Le Pichon *et al.* 1995; Chamot-Rooke *et al.* 2004). Combining the orientations of the Bannock and Battos tracks with the expected plate motion direction, Le Pichon *et al.* (1995) and Chamot-Rooke *et al.* (2004) predicted roughly 22 mm yr^{-1} of dextral shear, where the latter study made use of the more up-to-date relative motions (McClusky *et al.* 2000) than did the earlier study of Le Pichon *et al.* (1995). Detailed surface deformation mapping showed that much, if not all, of this dextral shear is taken up close to the wedge–backstop contact (Chamot-Rooke *et al.* 2004).

3 DESCRIPTION OF REGIONAL MODEL

Although the immediate focus of this study is the southern Aegean and in particular the MR, the region covered by our model stretches out from the Azores to the Caucasus and from the equator to central Europe. The major reason is to avoid edge effects, either related to the modelling approach or the inappropriate use of velocity boundary constraints, in our study of the southern Aegean.

In a large diffuse deformation zone such as the Mediterranean, it is appropriate to quantify the horizontal deformation field by using the principles of continuum mechanics. We use a well-established approach (Haines & Holt 1993) to obtain a horizontal velocity gradient tensor field. In this approach, model velocities are matched to observed velocities in a least-squares sense and then spherically expanded in terms of a rotation vector function using bi-cubic splines. A thorough discussion of the method is presented elsewhere (Holt *et al.* 2000; Beavan & Haines 2001). Earlier, the same general method has been used, and shown adequate, in the modelling of the horizontal kinematics of subduction zones (Kreemer *et al.* 2000) and, particularly appropriately, of a fold-and-thrust belt under oblique convergence (the Sulaiman Ranges of Pakistan) (Bernard *et al.* 2000).

To obtain a continuous velocity and strain rate field we defined a model grid. The grid consists of cells that are 0.5° by 0.6° in dimension. The plate boundary zones are covered by grid cells that are allowed to deform and a model strain rate tensor is then determined

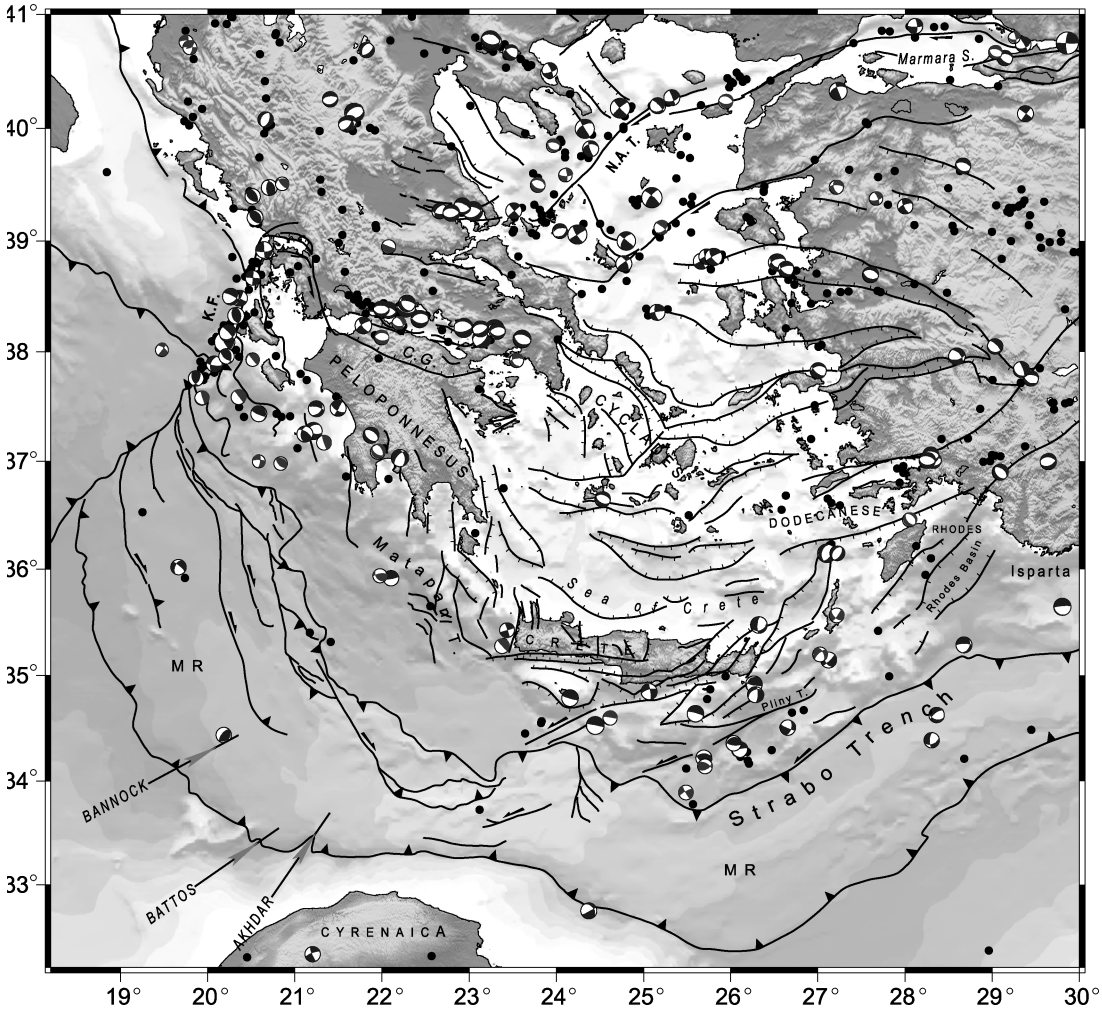

Figure 2. Active faults in the greater Aegean used to constrain the style of faulting in model B (from the DOTMED Group, Ecole Normale Supérieure). Superimposed are the shallow ($\leq$15 km) seismicity (dots; Engdahl *et al.* 1998) and earthquake focal mechanisms from ($4.5 \leq M_w < 5.5$; Pondrelli *et al.* 2002) and Harvard CMT catalogue ($M_w \geq 5.5$). Also shown are the directions of the Bannock, Battos and Akhdar seamount tracks. Corinth gulf (CG); Kephalonia fault (KF); Mediterranean ridge (MR); North Aegean trough (NAT).

for each deforming grid cell. On the other hand, a large number of the grid cells are constrained to behave rigidly (i.e. the derivatives of the rotation vector function are set to zero) in order to simulate the tectonic plates: Eurasia, Nubia, Anatolia and Arabia. *A priori* rigidity is not assumed for the Aegean block in the initial modelling, however the Aegean block is implicitly considered as being separate from the Anatolia block conforming with available GPS data (Papazachos 1999; McClusky *et al.* 2000).

4 MODEL A: GPS WITH MINIMUM OTHER CONSTRAINTS

We have set up a model, model A, in which we match model velocities to the observed GPS vectors. In order to be able to fit the GPS velocities, we need to assign *a priori* strain rate variances to each grid cell of the model. With two exceptions, we have assigned the same variance to all grid cells: this would be analogous to the assumption of uniform strength (or rheology) from one grid cell to another. The two exceptions are the MR, which is made relatively weaker ($\sim$2.5 times), and the region south of the wedge, which is made relatively stronger (*ca* 1.3 times; *cf* Bernard *et al.* 2000; Kreemer *et al.* 2000). The different treatment of these regions is partly based on expected lithological contrasts. The core of the MR is made of Neogene sediments plus an outward belt of Messinian evaporites, all deformable, and the region south of the deformation front is mainly rigid Mesozoic oceanic crust. For the purpose of this paper, the continental crust of Libya can be assumed to behave relatively rigid as well. The shape of the MR is taken from the bathymetry. The backstop of the western and eastern MR is assumed to be made of continental crust (Truffert *et al.* 1993). It should be stated that our goal is not to accurately model the effects of observed rheological contrasts in the accommodation of relative plate motions, but more to create a simple model that would illustrate (in the next section) the importance of including offshore kinematic indicators.

The model strain rate field and velocity field (with respect to Nubia) for model A are shown in Fig. 3. As expected, strain rates within the MR are large and approximately constant between the wedge–backstop contact and the deformation front. The direction of compressional strain rates is roughly parallel to the plate motions in the western MR, and roughly N–S in the eastern portion of the wedge, similar to the result by Kahle *et al.* (2000). High to moderate levels of shear strain rates are predicted near the Kephalonia fault

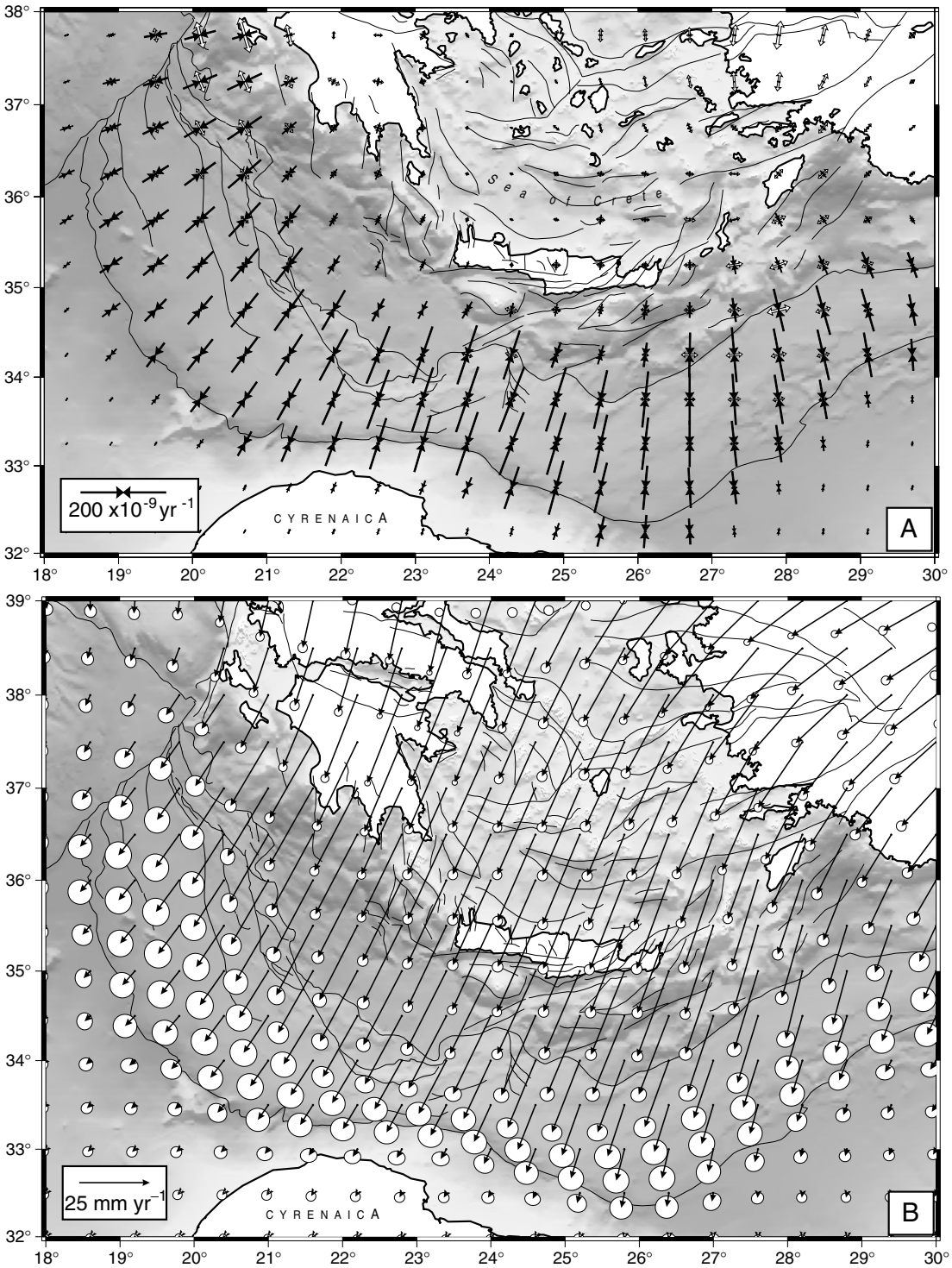

Figure 3. Results from model A, in which we have obtained a best fit between observed and model velocities and then calculated a continuous model strain rate and velocity field through a Bessel spline interpolation. No constraints from active faulting are included, but the MR and region south of the wedge are made respectively weaker and stronger than the continental crust of the Aegean. (a) Principal axes of the model strain rates, calculated as averages for each $0.5^\circ \times 0.6^\circ$ grid area and plotted at grid centers. White and black vectors are principal extensional and compressional strain rate axes, respectively. (b) Model velocities shown at grid knot points. Velocities are with respect to Nubia and error ellipses represent 95 per cent confidence ellipses.

zone and in the eastern MR (near the Strabo trench), respectively. It is an interesting observation that simply based on geometry and GPS/plate motions, shear is predicted in the eastern MR and not in the western portion of the wedge, conforming to previous strain rate models (Kahle *et al.* 1999, 2000).

We find that generally model A does not properly describe a range of known features of the wedge (Chamot-Rooke *et al.* 2004). First, shortening directions along the western deformation front are 10°–20° more northward than the seamount tracks suggest. Secondly, deformation rates along the crest of the wedge, where the sediment

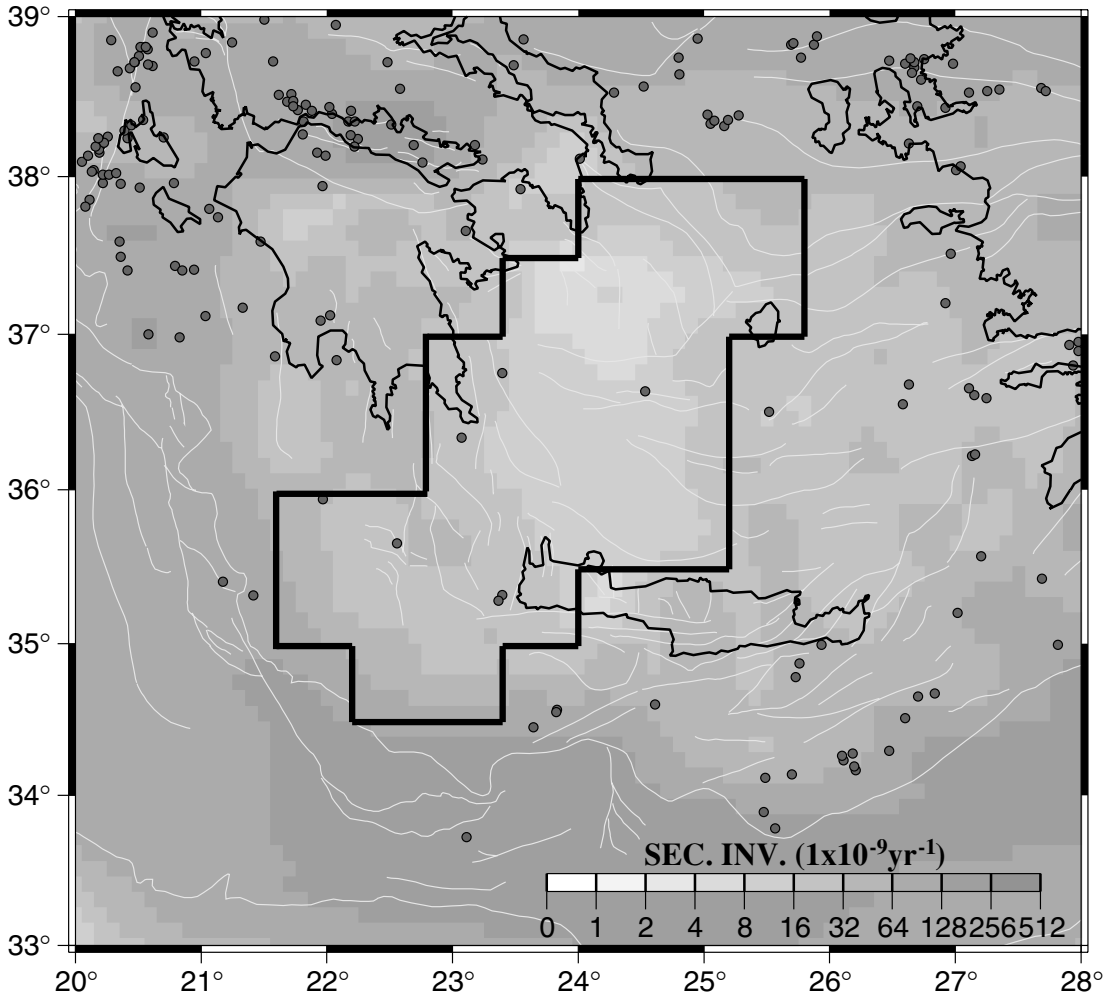

Figure 4. Contour plot of the second invariant of the model strain rates obtained in model A. Grey dots are locations of shallow (≤15 km) seismicity from Engdahl *et al.* (1998). White lines are active fault traces used in the model. Region outlined by black lines is *a priori* constrained to behave rigidly in subsequent model B.

layer is relatively thick and compacted, are expected to be relatively low compared to the deformation front and the region of the wedge–backstop contact, whereas the model predicts similar deformation rates everywhere in the wedge. Thirdly, shear at the wedge–backstop contact of the western arc, evidenced by observed flower structures and wrench tectonics, is not predicted by the model.

From the interpolation of GPS velocities, most of the Hellenic Arc and the south Aegean sea appear to deform relatively slowly at present, as was already concluded by others (Kahle *et al.* 1999; McClusky *et al.* 2000). Similar to Kahle *et al.* (2000), we find strain rates (Fig. 4) less than 0.005 μ strain yr^{-1} in the western Cyclades, Crete, the western and central sea of Crete, and within the wedge backstop of the western MR. These strain rates are quite similar to strain rates inferred within other rigid plates (Ward 1998a,b). The low deformation rate that we see for the backstop is the consequence of the fact we have constrained the backstop to have higher *a priori* strength than the MR. To facilitate the interpretation of results in the remainder of the paper, we have outlined in Fig. 4 the region that we wish to consider as one single rigid block (the Aegean block, or Aegea) in subsequent models. We do not include central and eastern Crete and the backstop of the eastern MR in the definition of the rigid block. For Crete, we do not want to *a priori* constrain its kinematics and for the eastern backstop there is ample evidence from seismicity (Fig. 2) and active faulting (Huchon *et al.* 1982) that this region is actively shearing.

5 HOW TO INCORPORATE FAULTING AND SEAMOUNT TRACK CONSTRAINTS?

To constrain the style, magnitude and distribution of the offshore (and to a lesser extent the onshore) deformation, we add information from active faulting (Fig. 2) to our inversion of the GPS velocity measurements. We design the *a priori* strain rate covariance matrix for each deforming grid cell such that it reflects the expected style (i.e. reverse, normal, or strike-slip, or any style intermediate) and direction of deformation for the fault (or faults) that are located within the grid cell. That is, following this methodology we are able to place constraints on the relative magnitude and direction of the expected principal strain rate axes. The constraint on direction involves an uncertainty of $\pm 10^{\circ}$. For the mathematical background behind this approach, see (Haines *et al.* 1998).

Next, we can also place constraints on the expected absolute magnitude of strain rate. For every active fault, we assume a weakness and this information is then reflected into the *a priori* strain rate

variances of the grid areas in which the faults are located. That is, the weaker a fault zone is believed to be, the higher we assign the *a priori* strain rates of the grid cells covering that fault and the more likely those cells will deform faster compared with others in the accommodation of the velocity field. The assigned strain rate variances range (in terms of corresponding slip rates) from 2 mm yr^{-1} for minor and presumed slowest faults to approximately 30 mm yr^{-1} for grid areas covering the NAF and the Kephalonia fault zones.

Some grid areas are not covered by one or more active faults. In most cases, these grid areas have been given a base variance corresponding to 1 mm yr^{-1} of expected motion over the grid cell and are thereby assumed to be relatively strong. Some of the grid cells not covered by faults are located along the crest of the MR where sediment thickness reaches a maximum and where the ridge is most compacted. By assigning the low base-level variance to these cells, we essentially mimic the more rigid nature of this region. As in model A, all grid cells south of the active wedge toe are given a very small *a priori* strain rate variance to simulate near plate rigidity.

On land, where there are generally many GPS velocity estimates, the importance of the definition of the *a priori* covariance matrix is inferior compared to the aim of finding a best fit between model and observed velocities. Offshore, however, constraints on the style and direction of deformation together with the relative assumed weakness from one zone to another become very important and determines to large extent our model results. Although the style of the offshore faults is generally well known and constrained by seismic and bathymetric data (Chamot-Rooke *et al.* 2004), the relative weakness of each fault (i.e. the amount of motion individual faults accommodate) is much more difficult to assess. We have tested several scenarios and present here our preferred solution that both corresponds best to the available data indicating which areas are deforming more than others (Chamot-Rooke *et al.* 2004) and is consistent with seamount track orientations.

As already discussed, we can use the track orientations to constrain the directions of the principal axes of the local convergent strain rate. We try to indirectly fit the direction of the principal convergence axis of the local model strain rate with the directions of the Bannock, Battos and Akhdar seamount tracks. This was done first by not constraining the active fault defining the wedge toe west of 24°E to a certain faulting style, as was done for all other faults. Assigning reverse faulting there would automatically constrain the convergence direction to be normal to the trend of the deformation front, which is inconsistent with the Battos and Akhdar track directions. Next, we assigned high enough *a priori* strain rate variances (with the relative components of he *a priori* strain rate tensor such that they favour dextral strike-slip) to the roughly NNW–SSE trending strike-slip faults within the western MR (Chamot-Rooke *et al.* 2004), such that the expected principal convergence direction near the seamounts matched the track directions best.

6 MODEL B: GPS WITH CONSTRAINTS FROM ACTIVE FAULTING AND SEAMOUNT TRACK DIRECTIONS

In our preferred model, model B, we have added the constraints from active faulting to the inversion of the set of GPS velocities. Horizontal model strain rate and velocity fields of the MR region at large are shown in Fig. 5: average horizontal strain rates for each 0.5° by 0.6° large area can be found in Fig. 5(a) and velocities with respect to NU and the backstop are shown in Fig. 5(b) and 5(c), respectively.

We are able to obtain a best fit between the directions of seamount tracks and compressional strain rates when the strain rate variance assigned to the NNW–SSE trending strike-slip faults between the ridge crest and the backstop is analogous to 19–23 mm yr^{-1} of dextral motion. This result is consistent with the value calculated by Le Pichon *et al.* (1995) and Chamot-Rooke *et al.* (2004). Although we attempt to fit the strain rate directions with the seamount tracks, we note that relative velocities near the seamount tracks in model B (Fig. 5b) are in agreement with the track directions, whereas there was no such agreement in model A (Fig. 3b).

6.1 Kinematics of the Aegean block and the Hellenic arc

Apart from fitting the newly added constraints, a major difference with model A is that we now include a rigid AE. The presence of a rigid southern Aegean was earlier shown by McClusky *et al.* (2000). For model B, the GPS and model velocities with respect to stable Aegea are shown in Fig. 6 for the southern Aegean. The weighted RMS is equal to 1.11 mm yr^{-1} between the model and observed velocities at the eight sites that are assumed to be situated on the AE. Within the 95 per cent confidence interval of the GPS velocities on the rigid block, all the eight sites move insignificantly with respect to the defined block. In the discussion, we will outline the existing evidence that the backstop of the western arc can be considered to be part of rigid Aegea as well.

Residual model velocities in Peloponnesus and southeast Aegean generally portray a small (1–5 mm yr^{-1} for Peloponnesus) to significant (up to ∼10 mm yr^{-1} for southeast Aegean) motion away from stable Aegea (Figs 5c and 6), consistent with what has previously been reported by others (Cocard *et al.* 1999; McClusky *et al.* 2000). For the southeastern Aegean, velocities progressively increase in speed towards the islands of Karpathos and Rhodes (McClusky *et al.* 2000) with particularly high extension rates along the Karpathos basin. This relative motion of the southeastern Aegean relative to Aegea is important in our study because it will change the velocity boundary condition for the two branches of the Hellenic arc.

The AE–EU angular velocity obtained from a best fit between model velocities and the eight GPS velocities measured on our defined Aegea can be described as a rotation rate of 0.33° Myr^{-1} about a pole at 43.4°S, 128.9°E (Table 2). Because the pole is located far from the microblock whose motion it describes, AE–EU relative motion can effectively be described as a translation of approximately 30–31 mm yr^{-1} in a S32°W ± 1° direction (Fig. 5b) consistent with the results of McClusky *et al.* (2000). We further find that the Aegea moves at 33–34 mm yr^{-1} towards S24°W ± 1° with respect to Nubia. The direction of NU–AE convergence is in agreement with the mean slip-vector direction of N21°E ± 10° deduced from low-angle thrust events along the subduction interface 35–40 km beneath Crete (Taymaz *et al.* 1990).

6.2 Deformation of the Mediterranean Ridge

The NU-fixed reference frame (Fig. 5b.) provides the best framework in which to describe both the relative motion between the overriding and downgoing plate (which is the appropriate velocity boundary condition), and the distribution of deformation within the wedge. The velocity field relative to the backstop (Fig. 5c), on the other

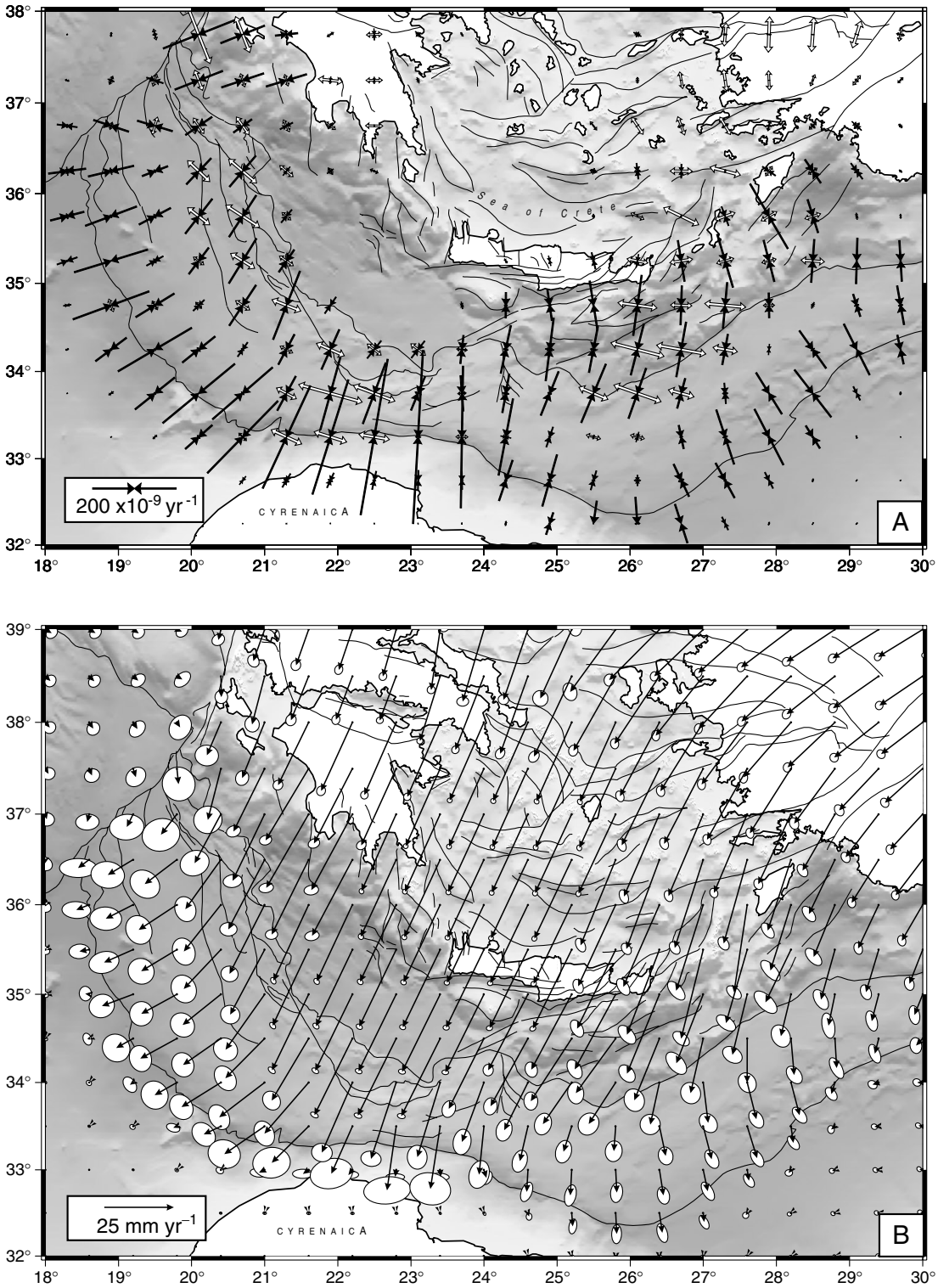

Figure 5. Results from model B, in which we have obtained a best fit between observed and model velocities and then calculated a continuous model strain rate and velocity field through a Bessel spline interpolation. Information on the location, style and relative weakness of the active faults in Fig. 2 are included as constraints in the interpolation. Seamount tracks (Fig. 2) are used to constrain local shortening direction (see text for details). (a) See Fig. 3(a). Along the MR, uncertainties in rate of strain are in the order of 20–30 per cent of the second invariant of the model strain rates. Uncertainties in the direction of the model principal strain axes are generally less than 15°; (b) see Fig. 3(b); (c) same as in (b), but model velocities are with respect to the backstop/Aegean block.

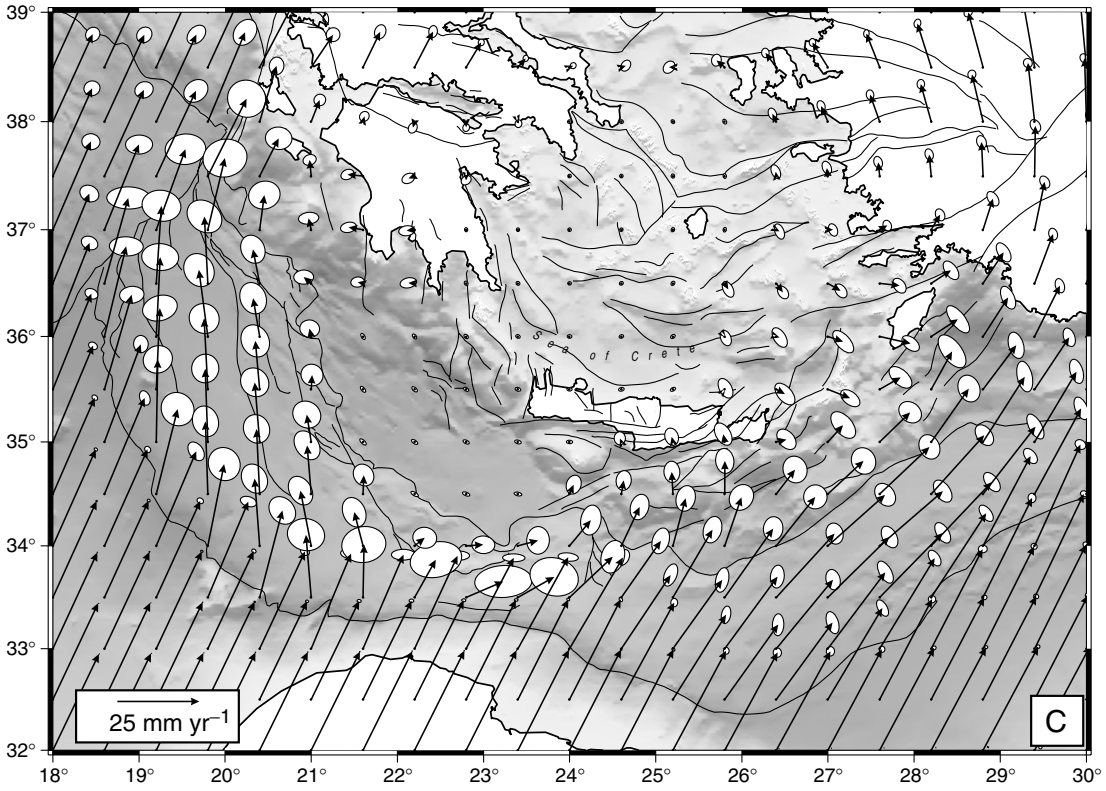

Figure 5. (*Continued.*)

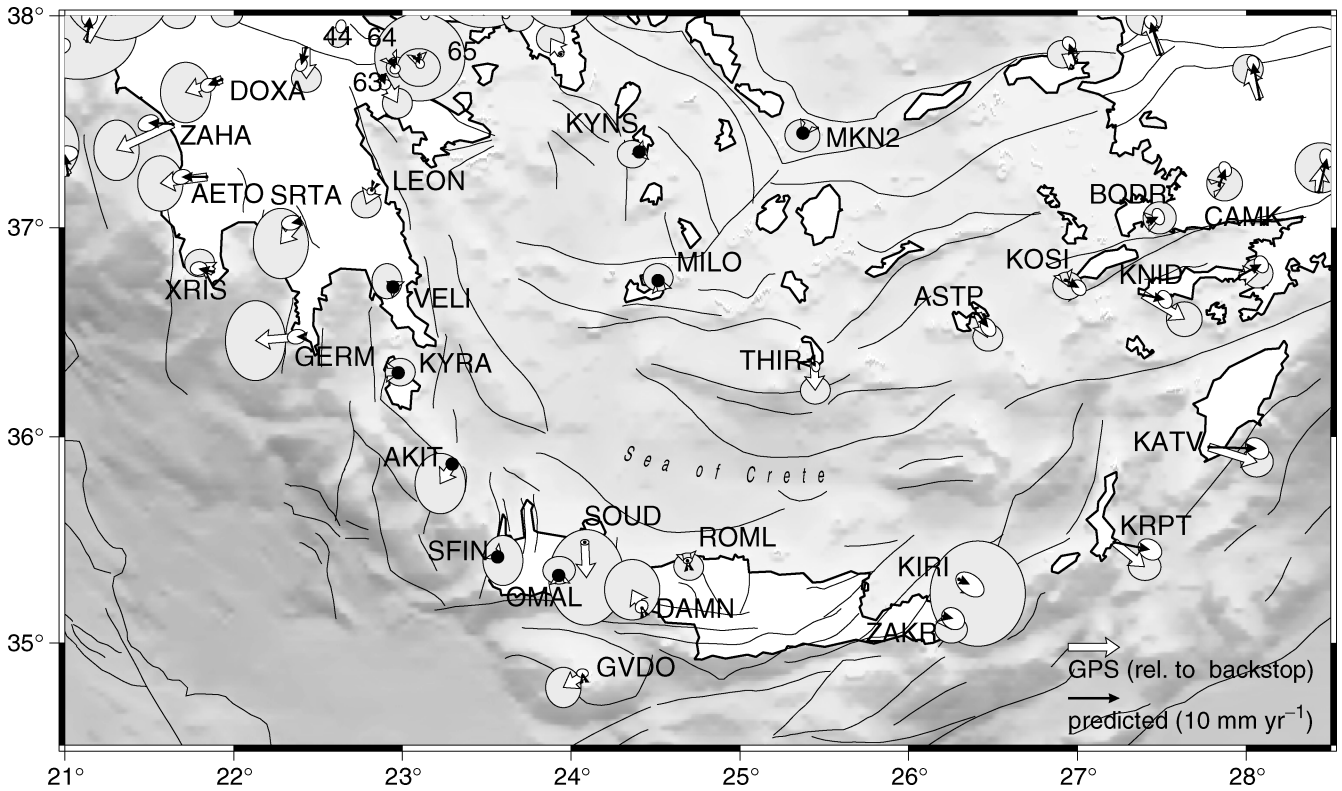

Figure 6. Model (black) and observed (white) velocities with respect to the defined AE. At sites that are assumed to be located on the AE, model velocities are shown as black dots. Error ellipses represent 95 per cent confidence.

hand, helps us to better understand the process of strain partitioning along the western and eastern branches of the MR.

Because of the relatively high relative motion between the Hellenic arc and the northern African margin, compressional strain rates dominate most of the MR. The Kephalonia fault zone undergoes pure shearing with a total right-lateral motion of at least 20 mm yr^{-1} towards S7°W between the western Peloponnesus and the (effectively) NU plate west of the fault zone. Evident elastic coupling and low resolution of our model do not allow us to determine whether all deformation is localized along the main fault or, as our model suggests, deformation is distributed over some minor structures east of the main fault as well. The recent work by Nielsen (2003) suggests the former. The southern continuation of the Kephalonia fault zone is not clear. In our model we see a low level of dextral shear down to 36°30'N with compressional axes oriented NE to ENE near the wedge–backstop contact and ESE in the region where the MR meets the Calabrian wedge (Fig. 5a). South of 36°30'N, significant dextral shear strain rates are present along and west of the wedge–backstop contact, and the total N–S right-lateral motion is equivalent to roughly 19–23 mm yr^{1} (Fig. 5c). West of the wedge crest, the convergence direction relative to NU is rotated to an approximate S65°W direction (west of 20°30'E; Fig. 5b) and in the ∼100 km between the wedge crest and the deformation front more than 70 per cent of the total shortening rate normal to the wedge–backstop contact is accommodated. The high shortening rate in the outer wedge amounts to 0.13–0.20 μ strain yr^{-1} ENE–WSW compressional strain rates along the deformation front (Fig. 5a). The slightly higher compression than extension rates in the shear zone suggest transpression at the wedge–backstop contact.

Just north of Cyrenaica, the deformation regime changes drastically. Here, the distance between the deformation front and the backstop is not only the shortest (∼75 km), it also appears that the wedge undergoes out-of-sequence thrusting (Chaumillon & Mascle 1997) while the frontal thrust can no longer propagate southward into the African continental margin (Chamot-Rooke *et al.* 2004). To accommodate 33–34 mm yr^{-1} shortening over such a short distance, compressional strain rates along the deformation front must be large (0.26–0.38 μ strain yr^{-1}; Fig. 5a). At the same time, the transition from right- to left-lateral shear, along the western and eastern MR, respectively, occurs in front of the Cyrenaica promontory. Consequently, NU–AE motion is diverted northward within the wedge west of Cyrenaica and to the northeast east of the promontory. This rapid E–W change in velocity direction requires relatively high extension in a roughly E–W direction and this, in combination with the high N–S convergent strain rates, gives rise to the high level of shear strain rates predicted between the backstop and Cyrenaica (Fig. 5a).

Along the deformation front east of Cyrenaica, the model strain rates are roughly the same magnitude as along the deformation front of the western MR, but the compression axes are oriented more NW to NNW, which is more normal to the wedge toe (Fig. 5a). Approximately 60 per cent of the total normal shortening rate is accommodated between the wedge crest and the deformation front. Consistent with the model constraints, the crest of the MR itself shows a low deformation rate. This reflects well the relative rigidity of the thick and compacted central portion of the accretionary wedge. Accommodation of the left-lateral motion within the eastern MR appears to be rather diffuse, but this may be merely the result of inappropriate (i.e. too large) grid spacing of the model. Deformation is observed to be localized onto the Pliny and Strabo trenches (Huchon *et al.* 1982; Huguen *et al.* 2001) and our model predicts left-lateral strike-slip motion of 21–23 mm yr^{-1} (Fig. 5c). This inferred rate is probably an upper limit. We have assigned pure strike-slip motion to the Pliny and Strabo trenches and have constrained deformation direction along the deformation front to be relatively normal to the wedge toe, thereby assuming full partitioning. It must be noted though that the strike-slip nature of the Pliny–Strabo trenches cannot be shown indisputably (Huchon *et al.* 1982). However, we argue that our assumptions on the presence of shear and partitioning are supported by the strain rate field of model A (Fig. 3b), which illustrates that, in the absence of offshore constraints, shear is predicted along the eastern MR simply as a result of the obliquity of the margin with respect to the convergence direction (model A placed the shear more in the wedge itself, because the wedge was assumed to be weaker than the backstop). The amount of strike-slip motion in model A over the Pliny and Strabo trenches is approximately 16 mm yr^{-1} and this may be considered to be a minimum rate.

South of central Crete, deformation is purely compressional and oriented roughly N–S. In Crete itself, the model predicts a very low level of NNW–SSE compression for the central part of the island and small E–W extension for the far eastern part. The Rhodes basin is under NW–SE compression with a minor shear component. This result contrasts with model A, in which the dominating style around Rhodes island was NE–SW extension (Fig. 3a). The large discrepancy between the two models for the expected strain rate style and magnitude is clearly the result from the imposed offshore faulting constraints; we have based the model constraint for the Rhodes basin on observed transpressional tectonics (ten Veen & Kleinspehn 2002). Ten Veen & Kleinspehn (2002) argued that at approximately 4–5 Ma a shift occurred from extension to sinistral strike-slip on to N70°E oriented faults as a result of the increasing obliquity of the convergent margin. It is believed that the present tectonic development of the Rhodes basin is in response to the propagation of the Pliny trench to the northeast (Woodside *et al.* 2000; ten Veen & Kleinspehn 2002).

7 DISCUSSION

7.1 Aegean block and Ionian backstop

Based on the geodetic measurements, we define a large portion of the southwest Aegean to be part of the same rigid block (Figs 4 and 6). From the GPS measurements, it also appears that Crete and Gavdos are part of rigid Aegea as well, although seismicity in and south of Crete (Lyon-Caen *et al.* 1988; Taymaz *et al.* 1990; Hatzfeld *et al.* 1993) and active faulting on Crete (e.g. Fassoulas 2001) suggest some level of active crustal deformation there.

The backstop of the western MR complex is a relatively rigid buttress comprised of Oligocene–Miocene carbonate nappes (Truffert *et al.* 1993). Le Pichon *et al.* (2002) argued that these nappes are the seaward extension of the Miocene Hellenic nappes found as outcrops in the southern Peloponnesus and Crete. Although a few small shallow earthquakes are known to have occurred along the Matapan trench (Fig. 2), the Harvard Centroid Moment Tensor (CMT) solutions and regional CMTs (Pondrelli *et al.* 2002) are inconsistent with each other: they exhibit strike-slip and low-angle reverse faulting at the same localities. In addition, one microseismicity survey (Hatzfeld *et al.* 1993) observed shallow ($z \leq$ 15 km) extensional (roughly E–W trending T-axis) and thrust (average NNE–SSW trending P-axes) earthquakes, offshore and onshore western Crete, respectively. Another survey (Jost *et al.* 2002) found that T-axes of shallow extensional and strike-slip events in western Crete trend roughly E–W. Hatzfeld *et al.* (1993) also recorded some

deeper ($20 \leq z \leq 30$ km) normal events southwest of Crete near the southeastern most extent of the Matapan trench with SE–NW trending T-axis. These latter events are consistent with present or very recent extension directions inferred from seismic profiles (Lallemant *et al.* 1994). The only significant event ($M_b = 5.8$) to have occurred northwest of Crete was the 1965 April 27 event, which had a pure E–W trending T-axis (Lyon-Caen *et al.* 1988) and that was thought to express arc-parallel extension. Nevertheless, we argue, based on the inconsistent style and low level of seismicity in combination with the GPS data, that the Matapan trench and western Crete do not delineate a significant active deformation zone and subsequently that the Ionian backstop is kinematically part of the AE. The reason why western Crete appears to be seismically relatively active, even though there is no evidence from GPS velocities that it is horizontally straining, may be the result of vertical motions associated with the subduction beneath Crete.

7.2 Strain partitioning and shortening in the Mediterranean Ridge

Two clear patterns emerge from the model velocity fields of the MR (Figs 5b and c). First, as already predicted by Le Pichon *et al.* (1995), with respect to the backstop the internal wedge moves away from Cyrenaica (Fig. 5c): the wedge moves northward NW of Cyrenaica and in a northeast direction NE of the promontory. Secondly, most of the outer wedge shortens in a direction that is different from the plate convergence direction: more westward west of Cyrenaica and more eastward east of the promontory (Figs 5a and b). Approximately 60–70 per cent of the plate velocity component normal to the leading edge of the backstop is accommodated by this shortening of the outer wedge. These patterns are consistent with the process of strain partitioning and are constrained by the observations of shear localization and seamount tracks that were used in this study. Partitioning along the Ionian branch of the MR is clearly required by the orientations of the seamount tracks (Chamot-Rooke *et al.* 2004). Although we have no reliable constraints on the shortening direction north of 34°30'N, the flower structures and wrench tectonics observed along the wedge–backstop contact provide evidence of partitioning to occur further north as well, but these structures do not give rate constraints. For the Herodotus branch, we partly constrained our model to a strain partitioning scenario by the input of strike-slip motion along the Pliny and Strabo trenches, and front-normal convergence along the deformation front. We believe that most of the constraints in the eastern MR are sensible. Active strike-slip deformation is observed along most of the Pliny and Strabo trenches (e.g. Huchon *et al.* 1982), significant shear is predicted by an unconstrained model (model A; Fig. 3a) and for a test model, in which we do not constrain the convergence along the wedge toe to be normal to the front, we observe roughly the same kinematic pattern. However, the degree of partitioning for the Herodotus branch remains somewhat unknown.

Oblique convergence is an obvious explanation for the pattern of strain partitioning, but it cannot fully explain the observed and predicted kinematic and tectonic pattern by itself. As a result of the sharp change in the trend of the Hellenic arc facing Cyrenaica, one would expect a local depression south of the backstop if strain partitioning occurs along both branches, because of the E–W extension related to the expected divergence between the western and eastern wedge. In reality, however, the region between Cyrenaica and the backstop is the shallowest portion of the entire wedge. The imminent collision between Cyrenaica and the MR has reached a stage where the frontal thrust facing Cyrenaica is no longer propagating southward because it has reached the African continental margin, and rapid shortening and uplift is occurring within the wedge by way of out-of-sequence thrusting. Thus, the expected depression north of Cyrenaica has been filled by the pre-collisional zone between the promontory and the backstop. Shortening and consequential uplift is so large that sediments are forced to flow away from this area, likely in the direction suggested by our model, as proposed by Le Pichon *et al.* (1995) (Fig. 5c). This lateral flow of the wedge with respect to the backstop thus partly enhances the effect of partitioning. If acting as the sole mechanism, lateral expulsion would however predict that the motion of the wedge away from the promontory, as well as the amount of shear along the wedge–backstop contact, would diminish with distance away from the collisional zone. In contrast, our model indicates that the inner wedge moves at roughly equal speed away from Cyrenaica (Fig. 5c). However, in our model we assume that shear occurs along most of the (Ionian) wedge–backstop contact and we are aware that north of 34°30'N the constraints on the amount of shear are less strong.

7.3 Outward growth rate of the Mediterranean prism

By using the well-studied Bannock seamount track and the model convergence rates, we are able to place bounds on the growth rate of the deformation front. The current deformation front is approximately 8 km outward from the paleo-location where the Bannock seamount entered the wedge (von Huene *et al.* 1997). The seamount track itself has grown to a length of approximately 42 km since the time the Bannock seamount entered the wedge, as result of the internal convergence of the wedge (von Huene *et al.* 1997). The rate of outward growth is thus approximately 20 per cent of the convergence rate. At the location of the Bannock seamount, the convergence rate with respect to NU is approximately 15 ± 2 mm yr^{-1} (Fig. 5c), which results in roughly 3 mm yr^{-1} propagation rate at the Bannock location. If we would assume that plate convergence and the rate of wedge build-up has been stable since the Bannock seamount entered the wedge, we would infer the time of entrance as 2.8 Ma.

Our rate estimate is probably a minimum because the wedge toe near the Bannock basin is less far propagated than it is at nearby locations. The shape of the deformation front is highly variable: the wedge has progressed further where there is a minimum of relief and a maximum sediment thickness in front of the wedge toe. Another reason why the actual propagation rate is probably faster than 3 mm yr^{-1} is because it now appears (Calais *et al.* 2003) that NU–EU motion has slowed down since at least 3.1 Ma, with an average rate over 3.1 Myr that is several mm yr^{-1} faster than the geodetically inferred present-day rate. It may thus be sensible to use a convergence rate at the Bannock seamount of 17–19 mm yr^{-1} instead of 15 mm yr^{-1} (assuming that internal deformation rates within the wedge have stayed constant over 2.8 Myr). As a result the growth rate would be closer to 4 mm yr^{-1}. A recent study (Kopf *et al.* 2003) estimated outward-growth rate based on four cross-sections through different sections of the MR. They found that the post-Messinian rate is between 0–7 mm yr^{-1}, consistent with our result.

7.4 Dynamic forces along the Hellenic arc

One of the foremost interests to quantify the crustal deformation field lies in the constraints it can provide to investigate the dynamics of the system. To this extent, particular focus has been given to the role of driving forces such as gravitational collapse, plate collision and slab retreat. Yet, despite all efforts to quantify the kinematics,

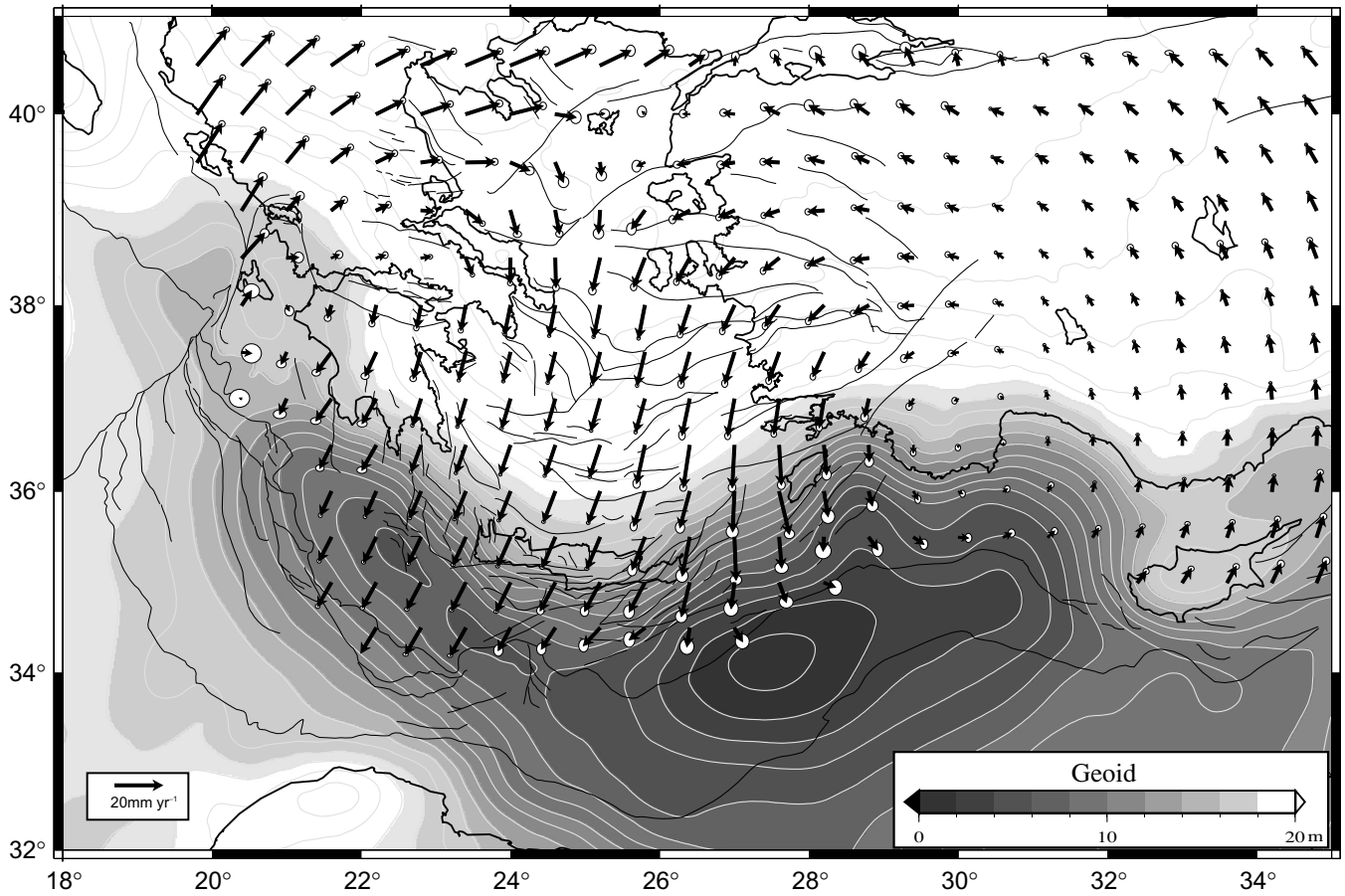

Figure 7. Model B velocities with 95 per cent confidence ellipses, superimposed onto a 2 m interval contour plot of the geoid height in the eastern Mediterranean. Only upper plate motion is shown. The chosen reference frame is such that the motion of the Hellenic arc is towards the geoid lows: SW for the Ionian branch and SE for the Herodotus branch. Note that the two anchor points, where the motion in this reference frame is zero, are located near the western and eastern extremities of the geoid anomaly.

debate still remains on the relative importance of the various driving forces behind the observed deformation pattern (e.g. Cianetti *et al.* 1997; Meijer & Wortel 1997; Lundgren *et al.* 1998; Mantovani *et al.* 2000; Martinod *et al.* 2000). It appears that most of the subtleties to distinguish between the different dynamic models can be found in the relative magnitude and directions of horizontal velocities in the southern Aegean (Le Pichon & Angelier 1979).

The two main characteristics of the kinematics of the southern Aegean are the rapid SSW motion of the rigid Aegea and the motion of up to 10 mm yr^{-1} of the southeastern Aegean away from stable Aegea (Fig. 5b and c) (McClusky *et al.* 2000). This motion has been the source of subsequent studies in which attempts have been made to explain this radial motion in a geodynamic context (Cianetti *et al.* 2001). To further explore the dynamics of the southern Aegean, we determine a new frame of reference in which the velocity field along the arc is constrained to point towards the geoid lows of the deep Mediterranean (Fig. 7). These geoid lows merely reflect mass deficit associated with the downgoing of the African plate and they reach their minimum values along the Ionian and Herodotus branches of the Hellenic subduction zone. The new reference frame shows the existence of two anchor points of the arc, off western Peloponnesus and off the Isparta angle in southern Anatolia. Both areas have little motion in the new frame and they correspond to the limits of the geoid lows at sea: these lows exist neither beyond the Kephalonia fault zone on the western side nor beyond Cyprus on the eastern side. We find that the new reference frame is not very different from an Anatolia fixed reference frame (McClusky *et al.* 2000). With respect to the anchor points, there is a motion of the arc towards the deepest portions of the western and eastern branch of the Hellenic trench (Fig. 7). Our result suggests that the divergence between the western and easternmost portion of the Hellenic arc can be explained by the mass deficits south of the arc. Regardless of whether the mass deficit at large is driving or maintaining the Aegea/Anatolia escape, or not, the detailed distribution of the mass deficit, particularly the open v-shape of the geoid anomaly, seems to be reflected in the near-field direction of motion of the arc.

Some studies have argued that the horizontal velocity field within the Aegean can be explained by potential energy differences within the overriding plate itself, leading to gravitational collapse (e.g. Davies *et al.* 1997; Hatzfeld *et al.* 1997; Martinod *et al.* 2000). Gravitational collapse would predict a continuous deformation field, with extension in zones of high potential energy and compression in regions with low potential energy (e.g. Jones *et al.* 1996). The rigid body rotation of the Aegean block, despite significant variations in crustal thickness as sources of potential energy differences, does not support a purely gravitational collapse mechanism in the upper plate. In the southeastern Aegean sea, on the other hand, the 10 mm yr^{-1} motion relative to Aegea is accommodated in a more diffuse fashion over the active grabens of the Dodecanese islands (with the

Karpathos basin as the most prominent feature). Thus, within the southeastern Aegean some component of the surface deformation field may also be explained as a result of density differences in the overriding plate itself. The extension directions in the overriding plate, however, are oriented in a roughly NW–SE direction (Fig. 5a), whereas the gravitational collapse model of Martinod *et al.* (2000) predicts a more NE–SW direction. It needs to be stated though that we have inferred directions for crustal strain rates, which are partly constrained by the orientations of the grabens, and the extension direction for the lithosphere as a whole may be different.

8 CONCLUSIONS

Our results can be summarized as follows:

(i) The directions of seamount tracks and information on active faulting place important constraints on the modelling of the style and distribution of deformation of the MR.

(ii) In the western MR, deformation accommodates approximately 19–23 mm yr^{-1} of dextral motion along NNW–SSE trending faults between the wedge crest and the wedge–backstop contact, where significant shear strain rates are predicted. For the eastern wedge sinistral motion of 21–23 mm yr^{-1} is taken up over the broad shear zone that includes the Strabo and Pliny trenches. High, near trench normal, strain rates occur along the deformation front with 60–70 per cent of the total convergence normal to the wedge–backstop contact taken up between the wedge crest and the wedge toe. For the western MR we inferred an outward-growth rate of approximately 4 mm yr^{-1}.

(iii) The wedge backstop and the southern Aegean sea can be considered as one single kinematic entity (the Aegean block) which exhibits insignificant internal deformation. The Aegean block moves consistently at 33–34 mm yr^{-1} towards S24°W $\pm$ 1° in an NU reference frame.

(iv) Our results suggest that the orientation of surface velocities in the southern Aegean are consistent with the gradients of the regional geoid anomaly, suggesting that an important driving force of the surface deformation lies offshore. Gravitational collapse as a result of density differences within the upper plate itself is not consistent with the fact that most of the southern Aegean deforms insignificantly. Some effect of gravitational collapse can not be dismissed for the southeastern Aegean.

ACKNOWLEDGMENTS

The authors thank C. Rangin, X. Le Pichon, W. Holt and J. Haines for help and constructive discussions and R. Reilinger and C. Ebinger (associate editor) for reviews.

REFERENCES

Ayhan, M.E., Demir, C., Lenk, O., Kilicoglu, A., Altiner, Y., Barka, A.A., Ergintav, S. & Ozener, H., 2002. Inter-seismic strain accumulation in the Marmara Sea region, *Bull. seismol. Soc. Am.,* **92,** 216–229.

Beavan, J. & Haines, J., 2001. Contemporary horizontal velocity and strain rate fields of the Pacific-Australian plate boundary zone through New Zealand, *J. geophys. Res.,* **106,** 741–770.

Bernard, M., Shen-Tu, B., Holt, W.E. & Davis, D.M., 2000. Kinematics of active deformation in the Sulaiman Lobe and Range, Pakistan, *J. geophys. Res.,* **105,** 13 253–13 279.

Biju-Duval, B., Letouzey, J. & Montadert, L., 1978. Structure and evolution of the Mediterranean basins, in *Initial Reports of the Deep Sea Drilling Project,* Vol. 142, Part 1, pp. 951–984, eds Hsü, K.J. & Montadert, L., U.S. Govt. Printing Office, Washington, DC.

Billiris, H. *et al.*, 1991. Geodetic determination of tectonic deformation in Central Greece from 1900 to 1988, *Nature,* **350,** 124–129.

Briole, P. *et al.*, 2000. Active deformation of the Corinth rift, Greece: results from repeated Global Positioning System surveys between 1990 and 1995, *J. geophys. Res.,* **105,** 25 605–25 625.

Calais, E., DeMets, C. & Nocquet, J.-M., 2003. Evidence for a post-3.16-Ma change in Nubia-Eurasia-North America plate motions?, *Earth planet. Sc. Lett.,* **216,** 81–92.

Chamot-Rooke *et al.,* 2001. Deep offshore Tectonics of the Mediterranean (DOTMED): A synthesis of Deep Marine Data in the Eastern Mediterranean. *DOTS Consortium Final Scientific Report, 17 AO Maps and 3 CD-ROMS*.

Chamot-Rooke, N., Rangin, C., Lallemant, S., Laurent, O., Le Pichon, X., Nielsen, C., Pascal, G. & Rabaute, A., 2004. Active tectonics of the Mediterranean Ridge, *Tectonics,* submitted.

Chaumillon, E. & Mascle, J., 1997. From foreland to forearc domains: new multichannel seismic reflection survey of the Mediterranean Ridge accretionary complex (Eastern Mediterranean), *Mar. Geol.,* **138,** 237–259.

Cianetti, S., Gasparini, P., Boccaletti, M. & Giunchi, C., 1997. Reproducing the velocity and stress fields in the Aegean region, *Geophys. Res. Lett.,* **24,** 2087–2090.

Cianetti, S., Gasparini, P., Giunchi, C. & Boschi, E., 2001. Numerical modelling of the Aegean-Anatolian region: geodynamical constraints from observed rheological heterogeneities, *Geophys. J. Int.,* **146,** 760–780.

Clarke, P.J. *et al.*, 1998. Crustal strain in central Greece from repeated GPS measurements in the interval 1989–1997, *Geophys. J. Int.,* **135,** 195–214.

Cocard, M., Kahle, H.G., Peter, Y., Geiger, A., Veis, G., Felekis, S., Paradissis, D. & Billiris, H., 1999. New constraints on the rapid crustal motion of the Aegean region: recent results inferred from GPS measurements (1993–1998) across the West Hellenic Arc, Greece, *Earth planet. Sc. Lett.,* **172,** 39–47.

Davies, R., England, P., Parsons, B., Biliris, H., Paradissis, D. & Veis, G., 1997. Geodetic strain of Greece in the interval 1892–1992, *J. geophys. Res.,* **102,** 24 571–24 588.

DeMets, C., Gordon, R.G., Argus, D.F. & Stein, S., 1994. Effects of recent revisions to the geomagnetic reversal time scale on estimates of current plate motions, *Geophys. Res. Lett.,* **21,** 2191–2194.

Engdahl, E.R., van der Hilst, R. & Buland, A.R., 1998. Global teleseismic relocation with improved travel times and procedures for depth determination, *Bull. seismol. Soc. Am.,* **88,** 722–743.

Fassoulas, C., 2001. The tectonic development of a Neogene basin at the leading edge of the active European margin: the Heraklion basin, Crete, Greece, *J. Geodyn.,* **31,** 49–70.

Fernandes, R.M.S., Ambrosius, B.A.C., Noomen, R., Bastos, L., Wortel, M.J.R., Spakman, W. & Govers, R., 2003. The relative motion between Africa and Eurasia as derived from ITRF2000 and GPS data, *Geophys. Res. Lett.,* **30**.

Fisher, D.M., Gardner, T.W., Marshall, J.S., Sak, S.B. & Protti, M., 1998. Effect of subducting sea-floor roughness on fore-arc kinematics Pacific coast, Costa Rica, *Geology,* **26,** 467–470.

Fruehn, J., Reston, T., von Huene, R. & Bialas, J., 2002. Structure of the Mediterranean Ridge accretionary complex from seismic velocity information, *Mar. Geol.,* **186,** 41–58.

Haines, A.J. & Holt, W.E., 1993. A procedure for obtaining the complete horizontal motions within zones of distributed deformation from the inversion of strain-rate data, *J. geophys. Res.,* **98,** 12 057–12 082.

Haines, A.J., Jackson, J.A., Holt, W.E. & Agnew, D.C., 1998. *Representing distributed deformation by continuous velocity fields, Sci. Rept. 9815,* Institute geol. nucl. Sci., Wellington.

Hatzfeld, D., Besnard, M., Makropoulos, K. & Hatzidimitriou, P., 1993. Microearthquake seismicity and fault-plane solutions in the southern Aegean and its geodynamic implications, *Geophys. J. Int.,* **115,** 799–818.

Hatzfeld, D., Martinod, J., Bastet, G. & Gautier, P., 1997. An analogue experiment for the Aegean to describe the contribution of gravitational potential energy, *J. geophys. Res.,* **102,** 649–659.

Holt, W.E., Shen-Tu, B., Haines, J. & Jackson, J., 2000. On the determination of self-consistent strain rate fields within zones of distributed deformation, in *The History and Dynamics of Global Plate Motions,* pp. 113–141, eds

Richards, M.A., Gordon, R. G. & van der Hilst, R.D., AGU, Washington, DC.

Huchon, P., Lyberis, N., Angelier, J., Le Pichon, X. & Renard, V., 1982. Tectonics of the Hellenic Trench: a synthesis of Sea-Beam and submersible observations, *Tectonophysics,* **86,** 69–112.

Huguen, C., Mascle, J., Chaumillon, E., Woodside, J.M., Benkhelil, J., Kopf, A. & Volkonskaia, A., 2001. Deformational styles of the eastern Mediterranean Ridge and surroundings from combined swath mapping and seismic reflection profiling, *Tectonophysics,* **343,** 21–47.

Jackson, J., Haines, J. & Holt, W., 1994. A comparison of satellite laser ranging and seismicity data in the Aegean region, *Geophys. Res. Lett.,* **21,** 2849–2852.

Jones, C.H., Unruh, J.R. & Sonder, L.J., 1996. The role of gravitational potential energy in active deformation in the southwestern United States, *Nature,* **381,** 37–41.

Jost, M.L., Knabenbauer, O., Cheng, J. & Harjes, H.P., 2002. Fault plane solutions of microearthquakes and small events in the Hellenic are, *Tectonophysics,* **356,** 87–114.

Kahle, H.G., Müller, M.V., Geiger, A., Danuser, G., Mueller, S., Veis, G., Billiris, H. & Paridissis, D., 1995. The strain field in NW Greece and the Ionian islands: results inferred from GPS measurements, *Tectonophysics,* **249,** 41–52.

Kahle, H.G. *et al.*, 1999. The GPS strain rate field in the Aegean Sea and western Anatolia, *Geophys. Res. Lett.,* **26,** 2513–2516.

Kahle, H.-G., Cocard, M., Peter, Y., Geiger, A., Reilinger, R., Barka, A. & Veis, G., 2000. GPS-derived strain rate field within the boundary zones of the Eurasian, African, and Arabian plates, *J. geophys. Res.,* **105,** 23 353–23 370.

Kastens, K.A., 1991. Rate of outward growth of the Mediterranean Ridge accretionary complex, *Tectonophysics,* **199,** 25–50.

Kopf, A., Mascle, J. & Klaeschen, D., 2003. The Mediterranean Ridge: A mass balance across the fastest growing accretionary complex on Earth, *J. geophys. Res.,* **108**.

Kotzev, V., Nakov, R., Burchfiel, B.C., King, R. & Reilinger, R., 2001. GPS study of active tectonics in Bulgaria: results from 1996 to 1998, *J. Geodyn.,* **31,** 189–200.

Kreemer, C. & Holt, W.E., 2001. A no-net-rotation model of present-day surface motions, *Geophys. Res. Lett.,* **28,** 4407–4410.

Kreemer, C., Holt, W.E., Goes, S. & Govers, R., 2000. Active deformation in eastern Indonesia and the Philippines from GPS and seismicity data, *J. geophys. Res.,* **105,** 663–680.

Kreemer, C., Holt, W.E. & Haines, A.J., 2003. An integrated global model of present-day plate motions and plate boundary deformation, *Geophys. J. Int.,* **154,** 8–34.

Lallemant, S., Truffert, C., Jolivet, L., Henry, P., Chamot-Rooke, N. & de Voogd, B., 1994. Spatial transition from compression to extension in the western Mediterranean Ridge accretionary complex, *Tectonophysics,* **234,** 33–52.

Le Pichon, X. & Angelier, J., 1979. The Hellenic arc and trench system: a key to the neotectonic evolution of the Eastern Mediterranean region, *Tectonophysics,* **60,** 1–42.

Le Pichon, X., Lybéris, N., Angelier, J. & Renard, V., 1982. Strain distribution over the Mediterranean Ridge: a synthesis incorporating new Sea-Beam data, *Tectonophysics,* **86,** 243–274.

Le Pichon, X., Chamot-Rooke, N., Lallemant, S., Noomen, R. & Veis, G., 1995. Geodetic determination of the kinematics of central Greece with respect to Europe: implications for eastern Mediterranean tectonics, *J. geophys. Res.,* **100,** 12 675–12 690.

Le Pichon, X., Lallemant, S., Chamot-Rooke, N., Lemear, D. & Pascal, G., 2002. The Mediterranean Ridge bachstop and the Hellenic nappes, *Marine Geology,* **186,** 111–125.

Lundgren, P., Giardini, D. & Russo, R., 1998. A geodynamic framework for eastern Mediterranean kinematics, *Geophys. Res. Lett.,* **25,** 4007–4010.

Lyon-Caen, H. *et al.*, 1988. The 1986 Kalamata (South Peloponnesus) Earthquake: detailed study of a normal-fault, evidences for east-west extension in the Hellenic arc, *J. geophys. Res.,* **93,** 14 967–15 000.

Mantovani, E., Viti, M., Albarello, D., Tamburelli, C., Babbucci, D. & Cenni, N., 2000. Role of kinematically induced horizontal forces in Mediterranean tectonics: insights from numerical modelling, *J. Geodyn.,* **30,** 287–320.

Martinod, J., Hatzfeld, D., Brun, J.-P., Davy, P. & Gautier, P., 2000. Continental collision, gravity spreading, and kinematics of Aegea and Anatolia, *Tectonics,* **19,** 290–299.

McClusky, S. *et al.*, 2000. Global Positioning System constraints on plate kinematics and dynamics in the eastern Mediterranean and Caucasus, *J. geophys. Res.,* **105,** 5695–5719.

McClusky, S., Reilinger, R., Mahmoud, S., Ben Sari, D. & Tealeb, A., 2003. GPS constraints on Africa (Nubia) and Arabia plate motions, *Geophys. J. Int.,* **155,** 126–138.

Meade, B.J., Hager, B.H., McClusky, S.C., Reilinger, R.E., Ergintav, S., Lenk, O., Barka, A. & Ozener, H., 2002. Estimates of seismic potential in the Marmara Sea region from block models of secular deformation constrained by global positioning system measurements, *Bull. seismol. Soc. Am.,* **92,** 208–215.

Meijer, P.T. & Wortel, M.J.R., 1997. Present-day dynamics of the Aegean region: a model analysis of the horizontal pattern of stress and deformation, *Tectonics,* **16,** 879–895.

Nielsen, C., 2003. Etude des zones de subduction en convergence hyperoblique; Ride Méditerranéenne, Marge Indo-Birmane, Université Orsay–Paris Sud, Paris, p. 206.

Noomen, R., Ambrosius, B.A.C. & Wakker, K.F., 1993. Crustal motions in the Mediterranean region determined from Laser Ranging to LAGEOS, in *Contributions of Space Geodesy to Geodynamics : Crustal Dynamics,* pp. 331–346, eds Smith, D.E. & Turcotte, D.L., AGU, Washington, DC.

Nyst, M.C.J., 2001. A new approach to model the kinematics of crustal deformation—with applications to the Aegean and Southeast Asia, *PhD thesis* Technische Universiteit Delft, Delft, p. 105.

Papazachos, C.B., 1999. Seismological and GPS evidence for the Aegean-Anatolia interaction, *Geophys. Res. Lett.,* **26,** 2653–2656.

Park, J.O., Tsuru, T., Kaneda, Y., Kono, Y., Kodaira, S., Takahashi, N. & Kinoshita, H., 1999. A subducting seamount beneath the Nankai accretionary prism off Shikoku, southwestern Japan, *Geophys. Res. Lett.,* **26,** 931–934.

Pondrelli, S., Morelli, A., Ekström, G., Mazza, S., Boschi, E. & Dziewonski, A.M., 2002. European-Mediterranean regional centroid-moment tensors: 1997–2000, *Phys. Earth planet. Int.,* **130,** 71–101.

Reilinger, R.E. *et al.*, 1997. Global Positioning System measurements of present-day crustal movements in the Arabia-Africa-Eurasia plate collision zone, *J. geophys. Res.,* **102,** 9983–9999.

Reston, T.J., Fruehn, J., von Huene, R. & IMERSE–Working-Group, 2002. The structure and evolution of the western Mediterranean Ridge, *Mar. Geol.,* **186,** 83–110.

Ryan, W.B.F., Kastens, K.A. & Cita, M.B., 1982. Geological evidence concerning compressional tectonics in the eastern Mediterranean, *Tectonophysics,* **86,** 213–242.

Sella, G.F., Dixon, T.H. & Mao, A., 2002. REVEL: A model for Recent plate velocities from space geodesy, *J. geophys. Res.,* **107,** 2081, 10.1029/2000JB000033.

Straub, C. & Kahle, H.G., 1994. Global positioning estimates of crustal deformation in the Marmara Sea region, Northwestern Anatolia, *Earth planet. Sci. Lett.,* **121,** 495–502.

Taymaz, T., Jackson, J. & Westaway, R., 1990. Earthquake mechanism in the Hellenic trench near Crete, *Geophys. J. Int.,* **102,** 695–731.

ten Veen, J.H. & Kleinspehn, K.L., 2002. Geodynamics along an increasingly curved convergent plate margin: Late Miocene-Pleistocene Rhodes, Greece, *Tectonics,* **21,** 10.1029/2001TC001287.

Truffert, C., Chamot-Rooke, N., Lallemant, S., de Voogd, B., Huchon, P. & Le Pichon, X., 1993. The crust of the Western Mediterranean Ridge from deep seismic data and gravity modelling, *Geophys. J. Int.,* **114,** 360–372.

von Huene, R., Reston, T., Kukowski, N., Dehghani, G.A., Weinrebe, W. & IMERSE Working-Group, 1997. A subducting seamount beneath the Mediterranean Ridge, *Tectonophysics,* **271,** 249–261.

Ward, S.N., 1998a. On the consistency of earthquake moment rates, geological fault data, and space geodetic strain: the United States, *Geophys. J. Int.,* **134,** 172–186.

Ward, S.N., 1998b. On the consistency of earthquake moment release and space geodetic strain, Europe, *Geophys. J. Int.,* **135,** 1011–1018.

Woodside, J., Mascle, J., Huguen, C. & Volkonskaia, A., 2000. The Rhodes Basin, a post-Miocene tectonic trough, *Mar. Geol.,* **165,** 1–12.

APPENDIX A: DETAILS ON INCLUDED GPS VELOCITIES

For various reasons we have removed several sites from the GPS data sets. We mention the most noteworthy removals here. Sites 9, 13, 16, 19, 30, 31, 42, 43, 54 and 59 from Clarke *et al.* (1998) were not used, because they all showed signs of transient motions. All sites published by McClusky *et al.* (2000) for which updated velocity estimates were presented by Meade *et al.* (2002) were not taken. Velocity estimates by Ayhan *et al.* (2002) at sites for which McClusky *et al.* (2000) and Meade *et al.* (2002) also presented velocities are not included. For sites at Chrisokellaria, Kithira and Roumelli, we only took velocity estimates from McClusky *et al.* (2000) and not from Cocard *et al.* (1999), because the latter study presented velocities measured over a shorter time span. For the site at Gavdos (the only GPS site south of Crete) we used the estimate of Cocard *et al.* (1999) because the estimate of McClusky *et al.* (2000) was from a shorter observation period. We did not use velocity estimates by Kahle *et al.* (1995) at sites for which Cocard *et al.* (1999) also presented velocities, with the exception of Matera and Dionysos.

Standard errors of velocity estimates were incorporated in the inversion. Uncertainties in the vectors of Cocard *et al.* (1999) have been multiplied *a priori* by a factor of two and of most estimates of Ayhan *et al.* (2002) by a factor of five. The published uncertainties of these studies are arguably smaller than what is realistic. Multiplying some uncertainties with a certain factor ensures that uncertainties for all GPS vectors are in the same order of magnitude.